

Studies on structural interaction and performance of cement composite using Molecular Dynamics

B.S. Sindu^{*1,2}, Aleena Alex¹ and Saptarshi Sasmal^{1,2}

¹Academy of Scientific and Innovative Research, India

²CSIR-Structural Engineering Research Centre, Taramani, Chennai-600113, India

(Received November 24, 2017, Revised January 31, 2018, Accepted February 2, 2018)

Abstract. Cementitious composites are multiphase heterogeneous materials with distinct dissimilarity in strength under compression and tension (high under compression and very low under tension). At macro scale, the phenomenon can be well-explained as the material contains physical heterogeneity and pores. But, it is interesting to note that this dissimilarity initiates at molecular level where there is no heterogeneity. In this regard, molecular dynamics based computational investigations are carried out on cement clinkers and calcium silicate hydrate (C-S-H) under tension and compression to trace out the origin of dissimilarity. In the study, effect of strain rate, size of computational volume and presence of un-structured atoms on the obtained response is also investigated. It is identified that certain type of molecular interactions and the molecular structural parameters are responsible for causing the dissimilarity in behavior. Hence, the judiciously modified or tailored molecular structure would not only be able to reduce the extent of dissimilarity, it would also be capable of incorporating the desired properties in heterogeneous composites. The findings of this study would facilitate to take step to scientifically alter the structure of cementitious composites to attain the desired mechanical properties.

Keywords: Molecular dynamics; C-S-H; cement clinkers; mechanical properties

1. Introduction

With the increase in infrastructural development, there is an exponential consumption of cement all over the world. Manufacture of cement accounts for approx. 5% of CO₂ emission thus contributing to a large share of global warming. Hence, it becomes utmost important to reduce the consumption of cement without sacrificing the growing demands in infrastructural development. This balance can be created only if the mechanical behavior of cement is completely understood and the properties that are deficient like low tensile strength and early crack propagation are improved. Improving even a percent of its tensile strength will lead to huge savings, both in terms of energy and economy (during production and operation). Though research is going on over decades to improve the tensile strength of cementitious composites, the efforts being made are trial and error based (Shannag 2000, Song and Hwang 2004). In order to efficiently improve the

*Corresponding author, Scientist, E-mail: sindu@serc.res.in

^a Principal Scientist, E-mail: saptarshi@serc.res.in

mechanical properties of cementitious composites, the load transfer mechanics of the material should be properly understood. To do so, fundamental structure and behavior of hardened cement paste should be properly analyzed and its performance under different types of loads should be understood. Thus, for better understanding the behavior (properties) of cement paste, it is essential to explore its structure–property relationship and to identify the key micro-structural parameters that play the significant role in the mechanical responses of cement paste.

Currently, conceptual understanding to relate the properties and mechanical performance of cementitious composites to its structural arrangement is complicated due to the presence of particles in a large range of length scales (from nanometer to millimeter). At the scale of micrometers, cement paste is comprised of unhydrated cement particles, hydration products (mainly of calcium silicate hydrate (C-S-H) gel and calcium hydroxide) and capillary pores. Research on cementitious composites is going on to understand the properties of different phases present at different length scales and how they interact with other phases. Velez *et al.* (2001) performed nano-indentation tests on cement clinkers in order to determine their mechanical properties like elastic modulus and hardness. Molecular dynamics (MD) simulations were also carried out to determine the properties of C-S-H (Pellenq *et al.* 2009, Hu *et al.* 2016). Micro-mechanical modeling of cement hydration was performed to determine the mechanical and transport properties of cement paste and mortar (Bullard *et al.* 2010, Bentz *et al.* 1994). It has been accepted that the tensile strength of concrete arises from the hydration products, importantly the cohesive property of C-S-H (Murray *et al.* 2010). The bonded and non-bonded interactions in C-S-H were reported as the major contributors to cohesive property. Therefore, it can be concluded that the atomic and molecular level interactions of C-S-H is mainly responsible for the strength and weakness of concrete.

Since, C-S-H is formed due to the hydration of cement clinkers, it also becomes important to understand the interactions of atoms in these molecular systems. In view of this, atomic and molecular level studies on cement clinkers and C-S-H would provide a helping hand in identifying the source of different properties observed at macro level and providing guidelines for tailoring its structure in order to get desired properties. A major challenge in evaluating the mechanical properties of C-S-H at molecular level is its complex and varied micro-structural arrangement consisting of ions and pores. The configuration of C-S-H is found to be similar to that of Tobermorite and Jennite because the interlayer distance of C-S-H is similar to that of both these minerals. Hence, the behavior of C-S-H can be understood from these mineral models.

Recent studies (Masoumi and Valipour 2016, Sindu and Sasmal 2015, Eftekhari and Mohammadi 2016, Jensen *et al.* 2016, Ioannidou *et al.* 2016) attempted to evaluate the behavior of materials using MD which indicate the importance and interest on studying the cementitious composites at fundamental level in order to broaden the scientific understanding. The results obtained from the MD simulations can further be used to determine the mechanical properties of cement based materials using microporomechanics and suitable upscaling techniques. The tensile strength and modulus of cement paste was determined using fracture energy principles by considering the defects at molecular level and analytical homogenization techniques [Zhou *et al.* (2016)]. Though there are some MD studies on cementitious composites, the method of analysis in these studies are so random and solution driven. For instance, different types of force-fields are used for different components though they contain similar atomic species (Al-Ostaz *et al.* 2010); the size of simulation box is also randomly chosen and the properties are not evaluated using standardized and converged parameters. Further, thorough discussion on modelling and computational issues associated with evaluation of the mechanical properties of complex and

multi-phased material like cementitious composites has not been adequately reported. To the authors knowledge, studies on the mechanical response of the clinkers and hydrated phases (at atomistic level) under both tension and compression and investigations on identifying the reasons behind any change in property due to type of loading which is very important to further engineer the material, is absent.

The present work aims at investigating the mechanical properties of unhydrated phases of cementitious composites and the change in properties in course of evolution to the later hydrated phase using MD. A thorough methodology has been discussed which can be used for analyzing any phase of cementitious composite. The stress-strain behavior has been observed in three orthogonal directions in order to evaluate the degree of isotropy. The behavior of these phases under tension and compression has been obtained. An in-depth analysis has been carried out to correlate the observed properties with its atomic structure. Also, an attempt has been made to identify the reason behind the difference in behavior under tension and compression. The findings of this study will give a direction towards tailoring the structure of cementitious composites to give improved properties.

2. Molecular Dynamics simulations

MD simulations were carried out using Large-scale Atomic/Molecular Massively Parallel Simulator (LAMMPS) [Plimpton (1995)] an open source code available online. (<http://lammps.sandia.gov>). MD simulations were carried out on few key components of cementitious composites like cement clinkers and C-S-H like structures.

2.1 Atomic structures used in MD simulation

Tricalcium silicate (C_3S) is the most important compound and is generally found to be about 55–65% of total mass of cement. The crystal structure of C_3S proposed by Golovastikov et al. (1975) is taken up for the present study. The structure is built up of SiO_4^{4-} tetrahedral interspersed with Ca^{2+} and O^{2-} ions. Dicalcium silicate or C_2S is another important constituent of Portland cement. C_2S also has several polymorphs: α - C_2S , β - C_2S and γ - C_2S . α - C_2S proposed by Heller (1952) is adopted in the study. The structure is made up of isolated SiO_4^{4-} tetrahedral and Ca^{2+} ions, which resembles strings of alternating Ca ions and SiO_4 tetrahedral since four of the eight Ca ions are positioned alternately above and below SiO_4 tetrahedral in the vertical direction.

C-S-H is an important product formed during cement hydration. It forms about 60-70% of the total hydration products. Unlike cement clinkers, which have well defined structures, the atomic structure of C-S-H is not well established since it is a semi-crystalline composite. Experiments revealed that C-S-H possesses layered structure in which the distance between layers is in the range of few nanometers which is similar to the atomic structures of minerals like Jennite and Tobermorite (Richardson 2008). Hence, in this study, the crystal structures of Jennite and Tobermorite are used to study the behavior of C-S-H. The crystal structure of Jennite proposed by Bonaccorsi *et al.* (2004) is adopted in the present study. It consists of edge-sharing calcium octahedra, silicate chains and few calcium ions in the center. Tobermorite crystal exists in three different lattice spacings, 9Å, 11Å and 14Å. The crystal structure of Tobermorite with lattice spacing of 9Å and 11Å were taken from the structure proposed by Merlino *et al.* (2000), Merlino *et al.* (1999), respectively. The crystal structure of Tobermorite with silicate chains having a lattice

spacing of 14Å is taken from the structure proposed by Bonaccorsi and Merlino (2005). The lattice parameters of the atomic structures taken up in this study are given in table 1.

The major difference between atomic structures of clinkers and cement hydrates is that, layered silicate chains and interstitial water molecules that are present in hydrates are not present in clinkers. In clinkers, individual silicate units are present at certain distances. Apart from the absence of water molecules, the atomic interactions of C₂S and C₃S can be considered to be similar to that of C-S-H since same types of atoms are involved in both cases. Hence, the same force-fields or potential functions (explained in Section 2.2) can be used for evaluating their properties.

2.2 Methodology

In the present study, the simulations are carried out using Buckingham, Coulomb and Stillinger-Weber potential. Buckingham potential is used to calculate the Pauli's repulsion and van der Waals non-bonded interactions. The general expression for Buckingham Potential is as follows.

$$\phi_{12}(r) = Ae^{-Br} - \frac{C}{r^6} \quad (1)$$

where A , B , C are the constants and r is the distance between the two atoms considered. The terms in Buckingham potential are attractive and repulsive terms, respectively. When we obtain the derivative of the potential with respect to r , in order to calculate the forces, we get a negative force from the first term representing attractive force and a positive force from the second term representing repulsive force. Coulomb potential is used to calculate the electrostatic non-bonded interactions which is given as

$$E_{Coulomb} = \frac{q_i q_j}{Dr_{ij}} \quad (2)$$

where, q_i and q_j are the partial charges on atoms i and j separated by a distance of r_{ij} and D is a constant. Bonded interactions are defined using Stillinger-Weber Potential. It has two terms taking into account two body and three body interactions.

$$E = \sum_i \sum_{j>i} \varphi_2(r_{ij}) + \sum_i \sum_{j \neq i} \sum_{k>j} \varphi_3(r_{ij}, r_{jk}, \theta_{ijk}) \quad (3)$$

$$\varphi_2(r_{ij}) = A_{ij} \epsilon_{ij} \left[B_{ij} \left(\frac{\sigma_{ij}}{r_{ij}} \right) p_{ij} - \left(\frac{\sigma_{ij}}{r_{ij}} \right) q_{ij} \right] e^{\left(\frac{\sigma_{ij}}{r_{ij} - a_{ij} \sigma_{ij}} \right)} \quad (4)$$

$$\varphi_3(r_{ij}, r_{jk}, \theta_{ijk}) = \lambda_{ijk} \epsilon_{ijk} [\cos \theta_{ijk} - \cos \theta_{0ijk}]^2 e^{\left(\frac{\gamma_{ij} \sigma_{ij}}{r_{ij} - a_{ij} \sigma_{ij}} \right)} e^{\left(\frac{\gamma_{ik} \sigma_{ik}}{r_{ik} - a_{ik} \sigma_{ik}} \right)} \quad (5)$$

where φ_2 is two body term and φ_3 is three body term. A , B , p , q , λ , ϵ , γ , σ are constants and r is the distance between two atoms and θ is the angle. After defining the interaction between atoms through potential functions, periodic boundary conditions (PBCs) are applied in all directions of the unit cell in order to simulate the bulk behavior of the material. PBCs are used to overcome the problems caused by boundary effects in the finite size of simulation box and to make the system behave like a semi-infinite one. Ewald summation is used for computing long-range electrostatic interactions in order to achieve faster convergence.

Table 1 Lattice parameters of Crystal Structures

Materials	a (Å)	b (Å)	c (Å)	α	β	γ
Dicalcium silicate	9.34	9.22	10.61	90°	90°	90°
Tricalcium silicate	11.67	14.24	13.72	105.5°	94.33°	90°
Jennite	10.576	7.265	10.931	101.3°	96.98°	109.65°
Tobermorite (9Å)	11.156	7.303	9.566	101.08°	92.83°	89.98°
Tobermorite (11Å)	6.735	7.385	22.487	90°	90°	123.25°
Tobermorite (14Å)	6.735	7.425	27.987	90°	90°	123.25°

First, the system is subjected to minimization using Conjugate gradient method. Then, it is subjected to equilibration. NPT conditions are used to equilibrate the system to maintain the temperature at 300K and pressure at 0 bars. Nose-Hoover thermostat and barostat are used for this purpose. Choosing a suitable damping parameter is one of the crucial steps in equilibration. Generally, it is suggested that the ratio of damping parameter and time step to be maintained as 100 for reliable results. However, it varies according to the system under consideration. For the systems considered in this study, it is found that a ratio of 10 is optimum. The equilibration stage is followed by the production stage during which the actual simulation takes place. During production, the box is deformed at a constant rate along one direction and the system is constrained with NPT conditions on other two directions. Time step of 0.1 femtoseconds is used for carrying out the simulations and it is carried out for 2000 picoseconds.

At each time step, the stress on the system is calculated for applied strain. The macroscopic stress of N atoms contained in a volume, V can be expressed as

$$\sigma = \frac{Nk_B T}{V} + \frac{\langle W \rangle}{3V} \quad (6)$$

where T is the temperature, k_B is the Boltzmann's constant. $\langle W \rangle$ is the ensemble average of the internal virial due to forces (includes all bonded and non-bonded interactions) acting between the atoms which is given as

$$W(r^N) = -3V \frac{dU}{dV} \quad (7)$$

where, U is the potential energy. In case of pair potentials, it takes the form

$$U(r^N) = \sum_{n \in Z^3} \sum_{i=1}^N \sum_{j>1}^N u(r_{ijn}) + \sum_{n \in Z^3} \sum_{i=1}^N u(r_{iin}) \quad (8)$$

$$r_{ijn} = |r_i - r_{jn}|, \quad r_{jn} = r_j + Hn \quad (9)$$

where, r_{jn} denotes the position of one of the periodic images of atom j . The restriction of the summation is chosen such that exactly one periodic image of each pair interaction is included. The second summation denotes the self-interactions between periodic images of same atom. The detailed explanation on calculating the stress can be found elsewhere (Thompson *et al.* 2009).

3. Results and discussions

Studies are conducted on cement clinkers (C_2S and C_3S) and cement hydrate like structures (Jennite and Tobermorite). From the atomic/crystal structures of the clinkers and minerals (summarily termed as composite hereinafter), it is evident that the structural configuration is considerably different in all three directions. Hence, stress-strain relationships are obtained in all three orthogonal directions to evaluate the degree of isotropy. Studies are performed on composites both under tension and compression. The stress-strain relationship is linear at the initial stages, attains a maximum peak representing the strength of the molecular system and then declines. Young's modulus for each of the clinkers and minerals is calculated from the linear portion of the stress-strain curve. In order to maintain the consistency in the results, the linear portion is taken from origin to 0.4 times the maximum stress.

3.1 Parametric studies

The simulations, in this study, are carried out for certain parameters. In order to frame a generalized and stable simulation technique, it becomes important to study the influence of important parameters like time step, strain rate and simulation box size which is supposed to affect the computationally obtained results. Time step is an important parameter in any dynamics simulation. However, as explained in section 2.2, an appropriate ratio of damping factor and time step should be maintained to get reliable results. Since damping ratio is kept constant, the time step is also kept constant in this simulation. The sensitivity of other parameters like strain rate and simulation box size on Jennite are typically studied which are described in further sections.

3.1.1 Strain rate

The strain rate is an important parameter in any simulation. A low strain rate is generally preferred since a higher strain rate provides less accurate results. In this study, the strain rate is varied from 0.02 to 0.0002 and stress-strain behavior (along weakest direction) under different strain rates is obtained which are shown in figure 1. It can be observed that though the stress-strain plots tend to be refined at increased strain rate, the trend of these curves is found to be similar. There are two prominent peaks in the curve which occurs at 0.1 and 0.3 strain in all three curves and the maximum value of stress (strength) attained is similar. But while using a smaller strain rate, it is found that the second peak is more prominent than the first peak. This difference in observation may be due to lesser resolution in the data capturing at higher strain rate.

3.1.2 Simulation box size

To evaluate the influence of computational size on the overall response of the material under axial loading (which is extremely crucial for molecular simulation to strike a balance between accuracy and huge computational demand), three different simulation box sizes are adopted, viz., 1x1x1 consisting of single unit cell, 2x2x2 consisting of 8 unit cells and 3x3x3 consisting of 27 unit cells as shown in Fig. 2.

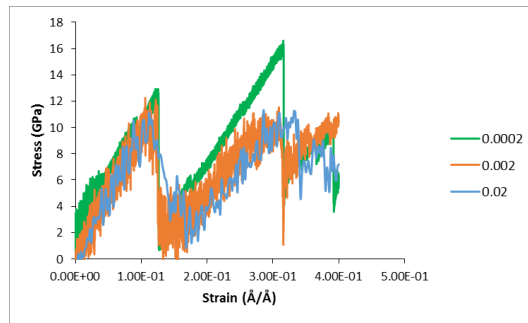


Fig. 1 Stress-strain relationship of Jennite under tension with different strain rates

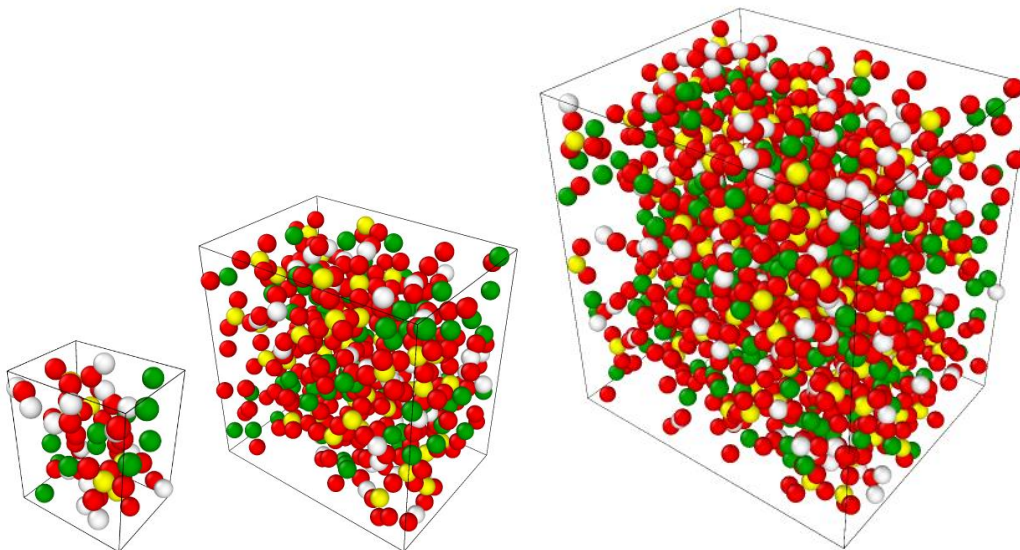


Fig. 2 Different simulation boxes of Jennite used for convergence study

Table 2 Comparison of results with different sizes of unit cell

Unit Cell	Young's Modulus (GPa)	Shahsavari <i>et al.</i> (2009)	Mohan <i>et al.</i> (2014)
1x1x1	61		
2x2x2	59	53	54
3x3x3	56		

As the number of atoms increase, the computation time also exponentially shoots up. Hence, the simulations are carried out for shorter periods of time and up to smaller strains in case of 2x2x2 and 3x3x3 as we aim to capture only the initial linear portion. The results are presented in table 2. It can be observed that as the simulation box size increases, the response becomes smoother and the predicted mechanical properties come closer to the established properties reported in the

literature. Hence, care was taken while choosing the simulation box size in order to create a balance between computational time and accuracy of results.

3.2 Tensile behavior

The simulation parameters are chosen based on the convergence of the parameters discussed above. The strain rate of 0.0002 is considered to get reasonably accurate results from the computational studies.

Dicalcium and Tricalcium Silicate

Stress-strain relationships of C_2S and C_3S in all three directions are shown in Fig. 3. From, these stress-strain relationships, the strength and Young's modulus of C_2S are found to be 14 GPa and 135 GPa, respectively. Similarly, strength of C_3S is observed to be 9 GPa and the Young's modulus is 123 GPa. The results obtained from the present study are validated with the values reported in the literature (table 3). It can also be found that the maximum stress is attained within a strain of 0.05 to 0.1 and the strength deteriorates completely within a strain value of 0.4. It can be noted that C_3S shows better isotropy than C_2S . It can also be observed from the figures that compared to C_2S , C_3S shows a more prominent linear behavior in initial stage. But, unlike C_2S , C_3S does not show distinct and clear peak stress (strength). This can be attributed to the presence of higher number of calcium ions present in the silicate matrix, which leads to increase in non-bonded interactions.

Discontinuity in stress-strain behavior

It can be seen that most of the stress-strain plots show sudden drops in stress value after it reaches maximum stress. When in some cases like C_2S , the stress loss is permanent and cannot be recovered after reaching the maximum stress, in few cases, stress increases again and the system continues taking more load. In order to understand the reason behind this behavior, typical stress-strain relationship of C_3S (as shown in Fig. 3(b)) is analyzed further. For this purpose, the distance moved by a single atom is monitored throughout the simulation. RMS distance of the atom under observation at the current time-step from the previous time-step is calculated and plotted. The units are scaled to the cell dimensions.

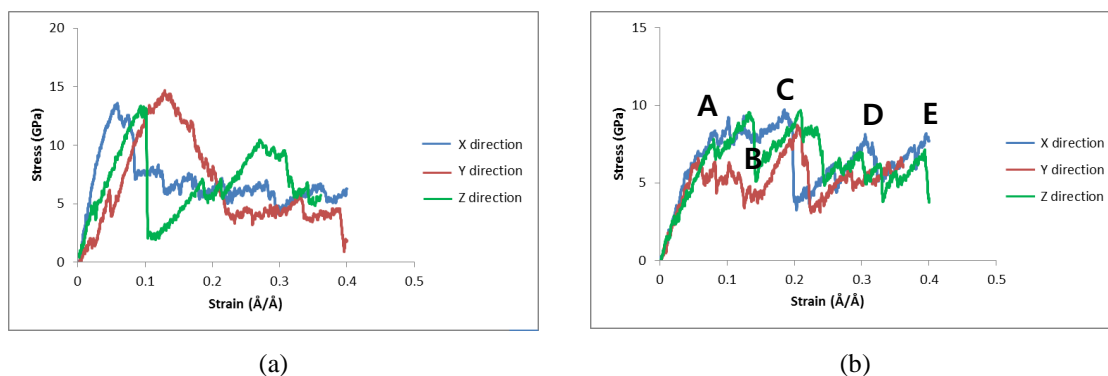


Fig. 3 Stress-strain relationships of (a) C_2S and (b) C_3S

Table 3 Validation of Young's Modulus of cement clinkers and minerals

Clinkers	Young's modulus (GPa)		
	Observed	Velez <i>et al.</i> (2001)	Wu <i>et al.</i> (2011)
C ₂ S	135	130 (SD 20)	121
C ₃ S	123	135 (SD 7)	137
Minerals	Observed	Shahsavari <i>et al.</i> (2009)	Plassard <i>et al.</i> (2010)
Jennite	47	53	--
Tobermorite 9Å	93	95	81
Tobermorite 11Å	90	83	
Tobermorite 14Å	47	52	--

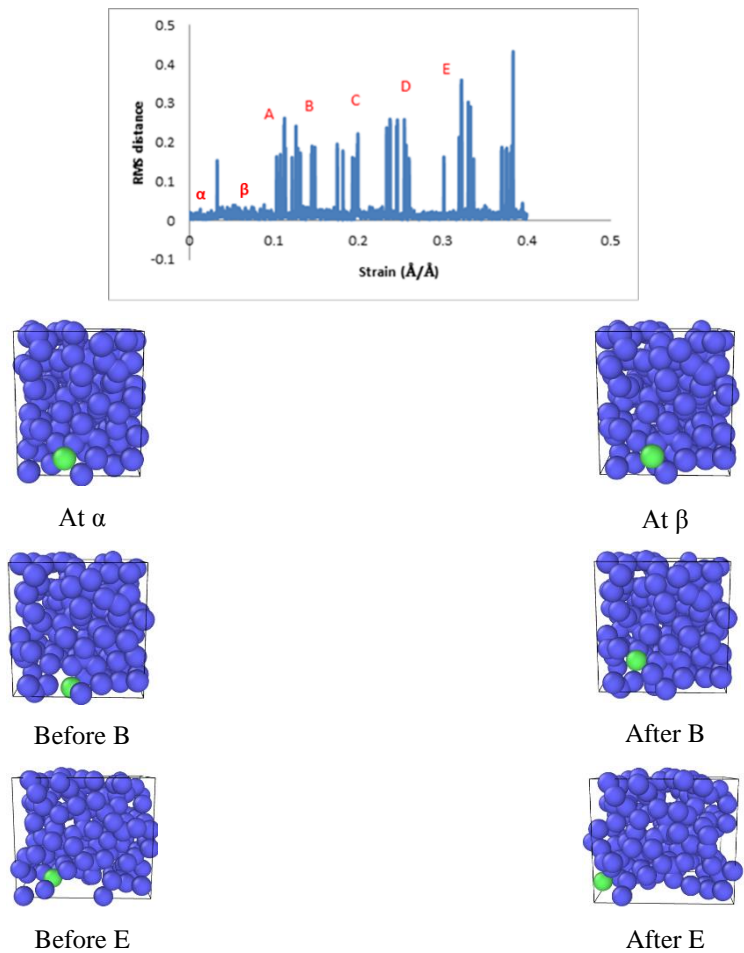


Fig. 4 RMS distance of a calcium atom with traces in crystal structure (with reference to Fig. 3(b)) where B and E depicts the large displacement

Few random atoms are selected and its RMS distance is compared with the stress-strain curve (Fig. 4). It can be observed that whenever there is a drop in stress-strain curve, there is a peak in the RMS distance, i.e., the atoms tend to have greater mobility at that point. This can also be explained as a drop in potential energy and an increase in kinetic energy. However, as the system is further loaded, the atoms rearrange themselves to a more stable order and are thus capable of taking further load. This may however be lesser than the maximum load taken earlier. Since periodic boundary conditions are assumed, the peaks in the RMS distance may also correspond to the atom moving out of a unit cell and another atom entering through its opposite side.

Cement hydrate like minerals (Jennite and Tobermorite)

Stress-strain behavior of Jennite in all three directions was obtained and strength and elastic modulus was found to be 7 GPa and 85 GPa (very close to the value reported by Al-Ostaz *et al.* 2010) respectively. Jennite also doesn't have a well-defined peak stress which is similar to that of C_3S behavior. It is to be noted that the strength and modulus of hydrated phase is lower than the clinker phase. This can be observed as the beginning of progressive reduction in mechanical properties which is further reflected in the micro level, viz., C-S-H gel and finally at the macro level viz., cement paste.

The crystal structure of Tobermorite is similar to that of Jennite where the silicate chains are arranged in layers. Based on the distance between the layers, three different Tobermorite crystals exist, i.e., Tobermorite (9Å), Tobermorite (11Å) and Tobermorite (14Å). The numbers inside the bracket denote the lattice spacing between silicate chains. It has been identified that the strength and Young's modulus of Tobermorite is not same in all three directions as observed in the previous case of cement clinkers. The strength of Tobermorite (9Å) varies from 7 GPa to 28 GPa and the Young's modulus varies from 93-250 GPa. The strength of Tobermorite (11Å) varies from 9 GPa to 25 GPa and the Young's modulus varies from 90-160 GPa. The strength of Tobermorite (14Å) varies from 7-25 GPa whereas the Young's modulus varies from 47-120 GPa. In order to determine the mechanical properties, the minimum value of strength and modulus is taken. The stress-strain curves are given in Fig. 5. The results obtained from the present study are validated with that reported in literature (presented in Table 3).

3.3 Compressive behavior

A homogenous material like aluminum or copper will exhibit similar stress-strain behavior in both compression and tension. But this is not the case for materials such as cementitious composite. It is well established that concrete is strong in compression and weak in tension. But, this behavior is observed in macro scale. In order to trace the source of this behavior, compressive studies are carried out on all the phases considered above.

The compressive strength of C_3S is obtained as 34 GPa and the Young's modulus is 200 GPa. The strength of C_3S is 17 GPa and Young's modulus is 122 GPa. The mechanical response under compression is found to be much superior than that observed under tension. There is a pronounced increase in both the properties under compression than that observed under tension (shown in Table 4), a phenomenon reflected in macro scale as well. Unlike tension, compressive strength degrades rapidly after a strain of 0.15. This may be due to a sudden and total distortion of molecular system, leading to failure.

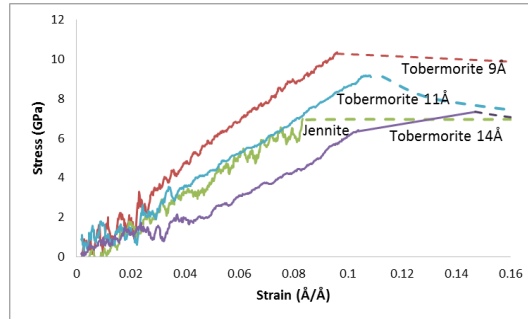


Fig. 5 Stress-strain relationship of hydrated minerals (solid lines – actual response, dotted lines – processed response)

Table 4 Comparison between uniaxial tension and compression results observed for C₂S, C₃S, Tobermorite and Jennite

Clinker/Mineral	Load type	Strength (GPa)	Young's Modulus (GPa)
C ₂ S	Tension	14	135
	Compression	34	200
C ₃ S	Tension	9	123
	Compression	17	122
Jennite	Tension	7	47
	Compression	13	86
Tobermorite (9Å/11 Å/14Å)	Tension	7/9/7	93/90/47
	Compression	40/18/10	200/167/87

The strength of Tobermorite with lattice spacing of 9Å, 11Å and 14Å are found to be 40 GPa, 18 GPa and 10 GPa, respectively and the Young's modulus is found to be 200 GPa, 167 GPa and 87GPa, respectively.

4. Investigations on difference in behavior under tension and compression

In order to identify the underlying difference in behavior under tension and compression, the composites are further analyzed. To bring out the relationship between structure of the composite with its behavior, analysis is carried out on three types of materials: (i) quartz, in which silicate units are fully bonded in all three directions, (ii) calcium silicates where silicate units, calcium atoms and water molecules are randomly distributed, and (iii) C-S-H like structure which has bonded and layered silicate chains along one direction and contains free calcium atoms and water molecules.

4.1 Influence on the type of molecular interactions

In all three types of materials, the contribution of different potentials towards the total stress of the composite (both under tension and compression) is identified. Since the contribution due to Stillinger-Weber (bonded) will remain same under tension and compression, it is not considered. The contribution of other two potentials, Coulomb (responsible for electrostatic interactions) and Buckingham (responsible for van der Waals interactions) potential is investigated. The change in energy of each potential at any strain level from its initial energy is plotted.

Quartz

The behavior of quartz is same under tension and compression as shown in Fig. 6(a). This is because in quartz, bonded interactions are more dominated than non-bonded ones.

Calcium silicates

It can be observed in Figs. 6(b) and 6(i) that the compressive strength (34 GPa) of C_2S is twice that of its tensile strength (14 GPa). It can also be observed from Fig. 6(b) (iii) that the change in

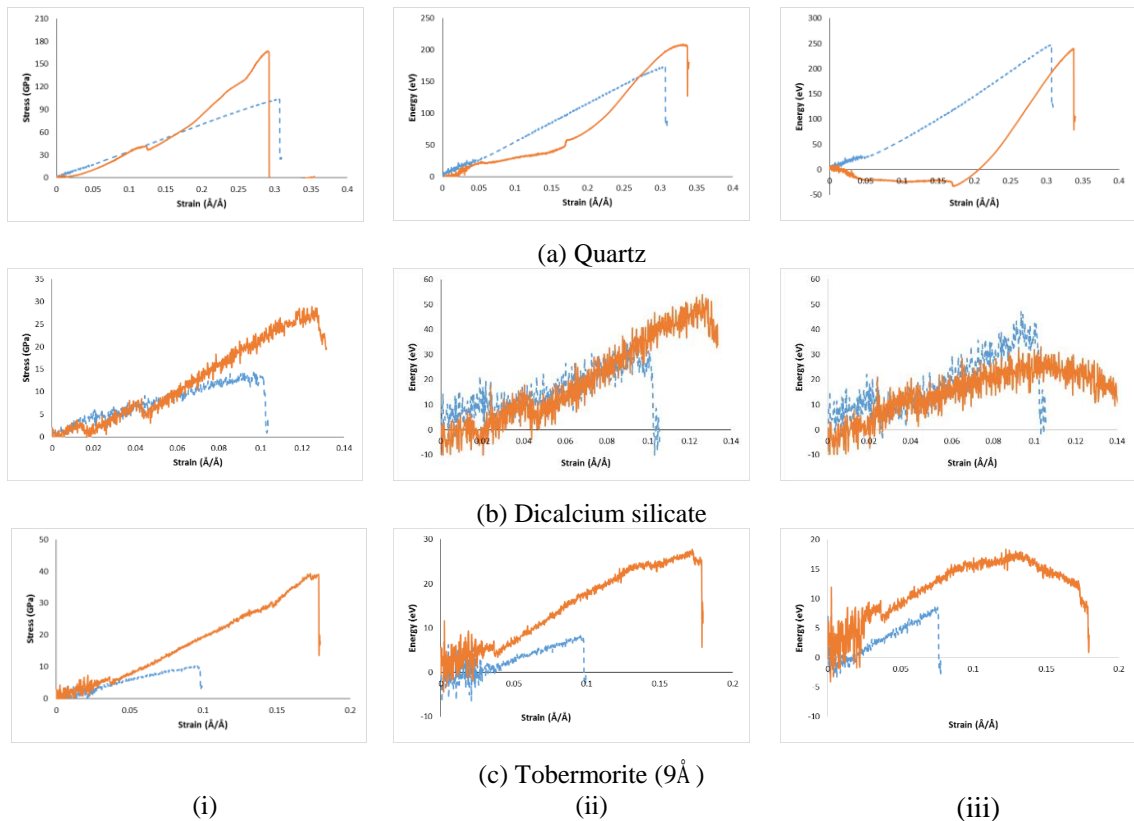


Fig. 6 (i) Stress-strain, (ii) Change in van der Waals energy and (iii) Change in electrostatic energy (— Compression, - - - Tension)

electro-static energy remains same under both tension and compression, whereas, change in van der Waals energy is less under tension when compared to that of compression (peak which is responsible for strength of the material).

C-S-H like structures

In case of Tobermorite (9\AA), the compressive strength (40 GPa) is five times greater than the tensile strength (7 GPa) [as observed in Figs. 6(c) and 6(i)]. Unlike calcium silicate, change in energy due to both the potentials is significant and both are contributing towards bringing the difference in behavior under tension and compression. However, change in stress due to van der Waals interactions is more predominant (3.5 times) as against electrostatic interactions (2.5 times). Hence, it can be concluded that van der Waals interaction is the major source of contribution for causing dissimilar behavior under tension and compression.

4.2 Influence on the molecular structural parameters

As it has been observed that C-S-H like structures exhibit more dissimilar behavior under tension and compression, an attempt has been made to identify the structural parameters responsible for causing the same.

4.2.1 Influence on lattice spacing

It can be observed from Table 4 that the tensile strength of tobermorite with different lattice spacings is almost the same. However, the compressive strength of the tobermorite decreases with the increase in lattice spacing. As the lattice spacing increases, not only the strength decreases, the modulus also decreases, i.e., the material becomes softer. From this, it can be noted that in order to get higher mechanical properties, the lattice spacing between silicate chains should be as low as possible.

4.2.2 Influence on the number of calcium atoms

The number of free calcium atoms available in interlayer of Tobermorite is varied. Two cases are considered: tobermorite enriched with calcium atoms and tobermorite deficient in calcium atoms (as shown in Fig. 7).

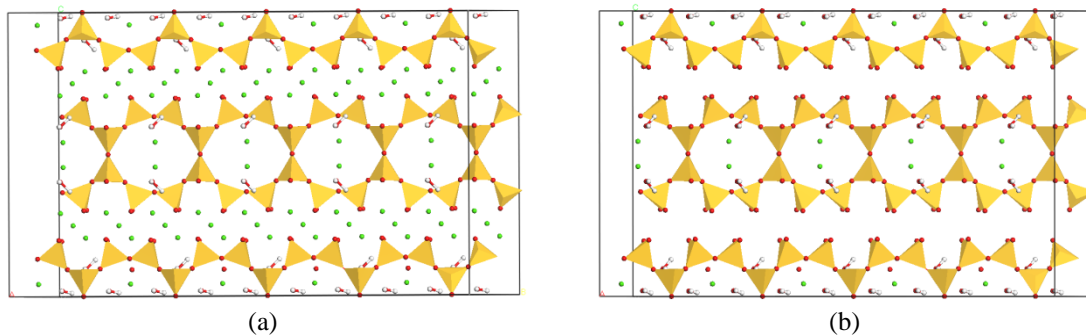


Fig. 7 Tobermorite (11\AA) (a) With extra inter-layer calcium atoms and (b) With less inter-layer calcium atoms

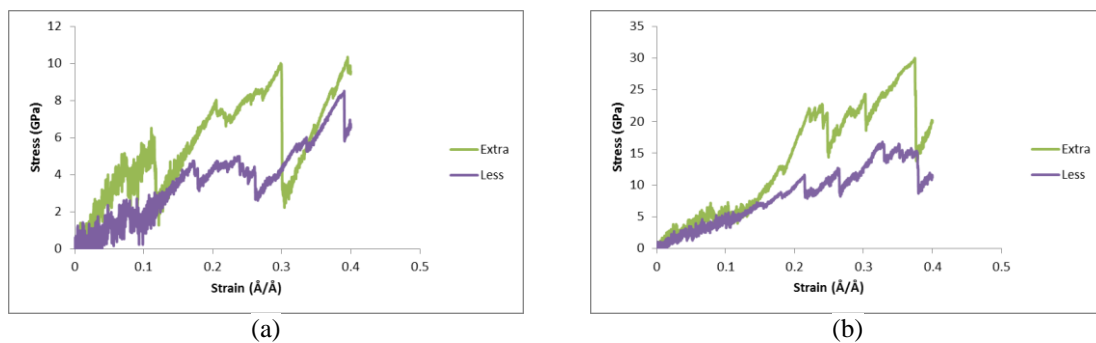


Fig. 8 Stress- strain plots of Tobermorite with extra and less calcium atoms under (a) Tension and (b) Compression

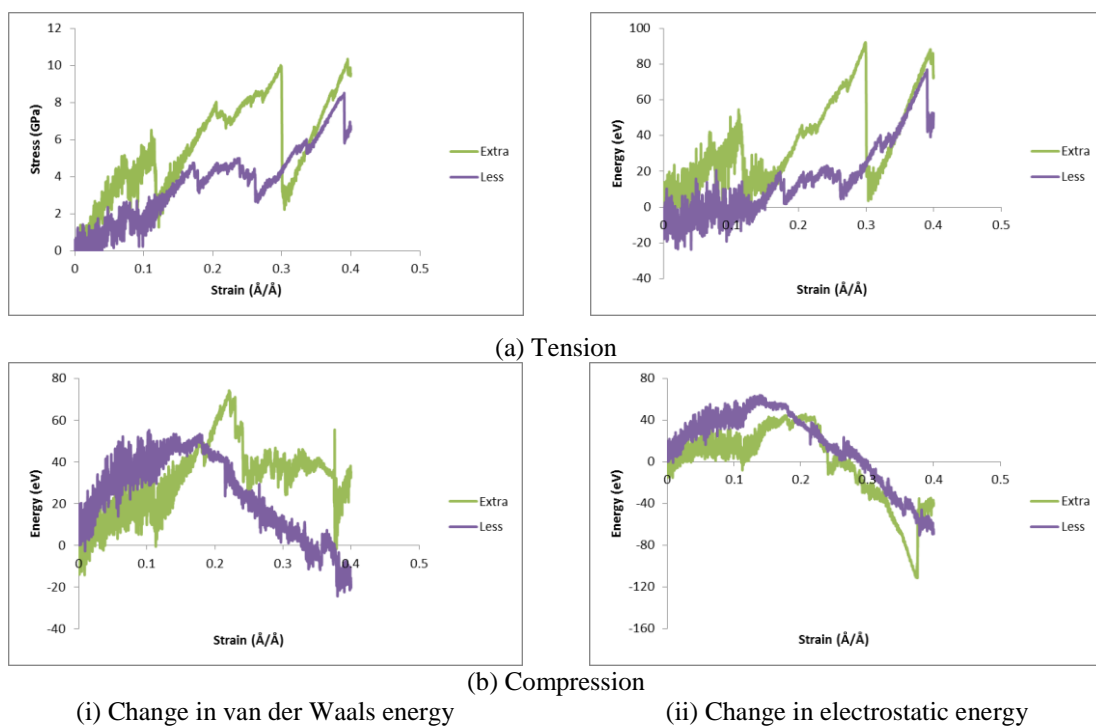


Fig. 9 Change in different non-bonded energies under tension and compression

The stress-strain behavior under tension and compression of both the cases are shown in Figs. 8 (a) and 8(b) respectively.

It can be observed that at strain 0.4 where the maximum stress (i.e., strength) is reached, the difference in stress between tobermorite of extra and less calcium atoms is not visible under

tension whereas there is a considerable difference in stress under compression. This indicates that the number of interlayer calcium atoms has no influence on the tensile strength whereas it significantly influences the development of the compressive strength. The type of non-bonded interactions responsible for this type of behavior can be identified from Fig. 9.

It can be observed from Fig. 9 that there is no change in electrostatic interactions as the number of calcium atoms is varied. However, there is a considerable change in van der Waals energy between both the configurations under compression. Hence it can be concluded that the presence of more free atoms leads to more discrepancy in behavior under tension and compression.

From the above results, the following observations can be made.

a) The discrepancy in behavior under tension and compression is less if the molecular system is predominated by bonded interactions.

b) If the molecular system contains more free atoms and molecules, non-bonded interactions become predominant and the discrepancy in behavior under tension and compression arises

The main reason for discrepancy in behavior under tension and compression is the variation in the number of atoms effectively contributing to stress under each case. For instance, number of contributing atoms in a microstructure (considering representative volume element, RVE) subjected to tension will decrease as the atom goes out of the cut-off distance. Whereas, under compression, the number of contributing atoms would not change as such. Hence, the peak stress (strength) is less in tension when compared to compression. Then it may be argued that all material systems will exhibit the similar phenomenon as discussed above. However, the question arises why some materials exhibit load sensitive mechanical responses (difference in behavior under tension and compression) while others do not.

Bonded interactions are not really sensitive to nature of loading. Hence, it is found that in materials where bonded interactions have more significant role on developed stress than that of non-bonded interactions, the response is found to be load insensitive.

The materials with layered microstructures and free atoms have significant contribution of non-bonded energy towards developed stress and in some cases, it exceeds the contribution of bonded energy. Hence, cement based materials with ample free atoms and inter-layer gap have the non-bonded interaction as major player to dictate the mechanical properties based on the nature of load.

Though this phenomenon is same for both the types of non-bonded interactions, the discrepancy is more only in the case of van der Waals interactions because the change of slope in van der Waals interactions is much steeper than the Coulombic one.

Hence, it can be concluded that the presence of free atoms and molecules and the layered structure are the major contributing parameters for cementitious materials showing discrepancy in behavior under tension and compression. This analogy also explains the reason for improved tensile strength, along with the desired improvement in compressive strength, in cement matrix improved through chemical intervention using reactive nano materials as reported (Nazari and Riahi 2011, Jalal *et al.* 2012). For example, though the reason of improvement of compressive strength of cement composite using nano silica was well reported and explained, the reason of improvement of tensile strength was not scientifically established. Addition of reactive nano materials (such as nano silica) enables to reduce the free calcium in the microstructure and restricts the microstructural inter-layer distance. Thus, the predominance of non-bonded interactions in the engineered microstructure is reduced. In this way, innovative nano/micro engineering of cement based materials for improved tensile strength is possible. This also enlightens that if the free atoms and molecules and the lattice spacing can be reduced by some means of chemical bonding, then the tensile strength of C-S-H can be brought closer to that of its compressive strength.

5. Conclusions

An attempt has been made in this study to understand the structure and behavior of various components of cementitious composites like cement clinkers and C-S-H like structures. Two major cement clinkers, C_2S and C_3S and C-S-H like structures, Jennite and Tobermorite (with different lattice spacing) have been subjected to constant strain to understand its mechanical characteristics. The sensitivity of parameters like strain rate and simulation box size on the stress-strain behavior is also analyzed. The results obtained from the present computational study are well corroborated with those from experimental and analytical studies. Further, it is interesting to note that the strength and Young's modulus of cement clinkers and hydration products under tension and compression are not equal. An in-depth computational investigation using the MD simulations is carried out to find out the parameters responsible for bringing out the discrepancy in behavior (response sensitive to the nature of load). It has been identified that micro-structures that are dominated by bonded interactions have similar compressive and tensile behavior. If the number of free atoms and molecular units is higher and if the lattice spacing is larger, the discrepancy in behavior also increases. Hence, it is suggested that in order to reduce the difference in behavior of C-S-H under tensile and compressive loading, the lattice spacing between silicate chains should be made lesser and some kind of chemical interventions would be made to lessen the free atomic and molecular units, and thereby achieve higher tensile strength.

References

- Al-Ostaz, A., Wu, W., Cheng, A.D. and Song, C.R. (2010), "A molecular dynamics and microporomechanics study on the mechanical properties of major constituents of hydrated cement", *Compos. Part B: Eng.*, **41**(7), 543-549.
- Bentz, D.P., Coveney, P.V., Garboczi, E.J., Kleyn, M.F. and Stutzman, P.E. (1994), "Cellular automaton simulations of cement hydration and microstructure development", *Model. Simul. Mater. Sci. Eng.*, **2**(4), 783.
- Bonaccorsi, E., Merlino, S. and Taylor, H.F.W. (2004), "The crystal structure of jennite, $Ca_9Si_6O_{18}(OH)_6 \cdot 8H_2O$ ", *Cement Concrete Res.*, **34**(9), 1481-1488.
- Bonaccorsi, E., Merlino, S. and Kampf, A.R. (2005), "The crystal structure of tobermorite 14 \AA (plombierite), a C-S-H phase", *J. Am. Ceram. Soc.*, **88**(3), 505-512.
- Bullard, J.W., Enjolras, E., George, W.L., Satterfield, S.G. and Terrill, J.E. (2010), "A parallel reaction-transport model applied to cement hydration and microstructure development", *Model. Simul. Mater. Sci. Eng.*, **18**(2), 025007.
- Eftekhari, M. and Mohammadi, S. (2016), "Molecular dynamics simulation of the nonlinear behavior of the CNT-reinforced calcium silicate hydrate (C-S-H) composite", *Compos. Part A: Appl. Sci. Manuf.*, **82**, 78-87.
- Golovastikov, N.I. (1975), "Crystal structure of tricalcium silicate, $3CaOSiO_2 = C_3S$ ", *Sov. Phys. Crystallogr.*, **20**, 441-445.
- Heller, L. (1952), "The structure of dicalcium silicate α -hydrate", *Acta Crystal*, **5**(6), 724-728.
- Hu, C., Gao, Y., Chen, B., Zhang, Y. and Li, Z. (2016), "Estimation of the poroelastic properties of calcium-silicate-hydrate (CSH) gel", *Mater. Design*, **92**, 107-113.
- Ioannidou, K., Kanduc, M., Li, L., Frenkel, D., Dobnikar, J., Pellenq, R. and Del Gado, E. (2016), "Gelation of calcium-silicate-hydrate in cement", *In APS Meeting Abstracts*.

- Jalal, M., Mansouri, E., Sharifipour, M. and Pouladkhan, A.R. (2012), "Mechanical, rheological, durability and microstructural properties of high performance self-compacting concrete containing SiO₂ micro and nanoparticles", *Mater. Design*, **34**, 389-400.
- Jensen, B.D., Wise, K.E. and Odegard, G.M. (2016), "Simulation of mechanical performance limits and failure of carbon nanotube composites", *Model. Simul. Mater. Sci. Eng.*, **24**(2), 025012.
- Masoumi, S. and Valipour, H. (2016), "Effects of moisture exposure on the crosslinked epoxy system: an atomistic study", *Model. Simul. Mater. Sci. Eng.*, **24**(3), 035011.
- Merlino, S., Bonaccorsi, E. and Armbruster, T. (1999), "Tobermorites: Their real structure and order-disorder (OD) character", *Am. Min.*, **84**(10), 1613-1621.
- Merlino, S., Bonaccorsi, E. and Armbruster, T. (2000), "The real structures of clinotobermorite and tobermorite 9 Å", *Eur. J. Mineral.*, **12**(2), 411-429.
- Mohan, R., Jadhav, V., Ahmed, A., Rivas, J. and Kelkar, A. (2014), "Effect of plasticizer additives on the mechanical properties of cement composite—a Molecular Dynamics analysis", *WASET, Inter. J. Chem. Mol. Nucl. Mater. Metal. Eng.*, **8**(1), 84-88.
- Murray, S., Subramani, V., Selvam, R. and Hall, K. (2010), "Molecular dynamics to understand the mechanical behavior of cement paste", *J. Transp. Res Board*, **2142**, 75-82.
- Nazari, A. and Riahi, S. (2011), "The effects of SiO₂ nanoparticles on physical and mechanical properties of high strength compacting concrete", *Compos. Part B: Eng.*, **42**(3), 570-578.
- Pellenq, R.J.M., Kushima, A., Shahsavari, R., Van Vliet, K.J., Buehler, M.J., Yip, S. and Ulm, F.J. (2009), "A realistic molecular model of cement hydrates", *Proc. Natl. Acad. Sci.*, **106**(38), 16102-16107.
- Plassard, C., Lesniewska, E., Pochard, I. and Nonat, A. (2007), "Intrinsic elastic properties of Calcium Silicate Hydrates by nanoindentation", *Proceedings of the 12th Inter. Cong. Chem. Cem.*
- Plimpton, S. (1995), "Fast parallel algorithms for short-range molecular dynamics", *J. Comput. Phys.*, **117**(1), 1-19.
- Richardson, I.G. (2008), "The calcium silicate hydrates", *Cement Concrete Res.*, **38**(2), 137-158.
- Shahsavari, R., Buehler, M.J., Pellenq, R.J.M. and Ulm, F.J. (2009), "First-principles study of elastic constants and interlayer interactions of complex hydrated oxides: Case study of tobermorite and jennite", *J. Am. Ceram. Soc.*, **92**(10), 2323-2330.
- Shannag, M.J. (2000), "High strength concrete containing natural pozzolan and silica fume", *Cem. Concr. Compos.*, **22**(6), 399-406.
- Sindu, B.S. and Sasmal, S. (2015), "Evaluation of mechanical characteristics of nano modified epoxy based polymers using molecular dynamics", *Comput. Mater. Sci.*, **96**, 146-158.
- Song, P.S. and Hwang, S. (2004), "Mechanical properties of high-strength steel fiber-reinforced concrete", *Constr. Build. Mater.*, **18**(9), 669-673.
- Thompson, A.P., Plimpton, S.J. and Mattson, W. (2009), "General formulation of pressure and stress tensor for arbitrary many-body interaction potentials under periodic boundary conditions", *J. Chem. Phys.*, **131**(15), 154107.
- Velez, K., Maximilien, S., Damidot, D., Fantozzi, G. and Sorrentino, F. (2001), "Determination by nanoindentation of elastic modulus and hardness of pure constituents of Portland cement clinker", *Cem. Concr. Res.*, **31**(4), 555-561.
- Wu, W., Al-Ostaz, A., Cheng, A.H.D. and Song, C.R. (2011), "Computation of elastic properties of Portland cement using molecular dynamics", *J. Nanomech. Micromech.*, **1**(2), 84-90.
- Zhou, J., Huang, J. and Jin, L. (2015), "Nano–micro modelling of mechanical properties of cement paste based on molecular dynamics", *Adv. Cem. Res.*, **28**(2), 73-83.